

BLASX: A High Performance Level-3 BLAS Library for Heterogeneous Multi-GPU Computing

Linnan Wang*, Wei Wu†, Jianxiong Xiao‡, and Yi Yang§

* Georgia Institute of Technology

† The University of Tennessee, Knoxville

‡ Princeton University

§ NEC Laboratory

Abstract—Basic Linear Algebra Subprograms (BLAS) are a set of low level linear algebra kernels widely adopted by applications involved with the deep learning and scientific computing. The massive and economic computing power brought forth by the emerging GPU architectures drives interest in implementation of compute-intensive level 3 BLAS on multi-GPU systems. In this paper, we investigate existing multi-GPU level 3 BLAS and present that 1) issues, such as the improper load balancing, inefficient communication, insufficient GPU stream level concurrency and data caching, impede current implementations from fully harnessing heterogeneous computing resources; 2) and the inter-GPU Peer-to-Peer (P2P) communication remains unexplored. We then present BLASX: a highly optimized multi-GPU level-3 BLAS. We adopt the concepts of algorithms-by-tiles treating a matrix tile as the basic data unit and operations on tiles as the basic task. Tasks are guided with a dynamic asynchronous runtime, which is cache and locality aware. The communication cost under BLASX becomes trivial as it perfectly overlaps communication and computation across multiple streams during asynchronous task progression. It also takes the current tile cache scheme one step further by proposing an innovative 2-level hierarchical tile cache, taking advantage of inter-GPU P2P communication. As a result, linear speedup is observable with BLASX under multi-GPU configurations; and the extensive benchmarks demonstrate that BLASX consistently outperforms the related leading industrial and academic projects such as cuBLAS-XT, SuperMatrix, MAGMA and PaRSEC.

Keywords—BLAS, scheduling runtime, tile algorithms, multiGPUs, hierarchical tile caches

I. INTRODUCTION

Matrix scaling, additions and multiplications are basic operations in linear algebra libraries, scientific simulations and deep learning. Offloading these operations to the BLAS library, which is the case in general practices, can substantially improve the application performance due to the architecture specific optimizations inside BLAS kernels. This leads BLAS to become the standard building blocks for performing low level matrix operations in applications. Hence, the BLAS library directly affects the application performance. In the last few years, the evolving GPU architectures, NVIDIA’s Kepler and Maxwell in particular, feature thousands of stream processors, proven to be extremely efficient in computing level 3 BLAS.

While a multi-GPU system offers appealing high performance, using it entails nontrivial effort. A multi-GPU system typically consists of at least one CPUs connected with peripheral GPUs on the PCI-E. GPU operates on its private onboard RAM while CPU operates on the host RAM. For GPUs sharing

the same I/O hub, they can directly communicate via PCI-E switch referred to as GPU P2P access. The following factors need to be considered to fully utilize such architecture: (1) nowadays GPUs of different architectures represent divergent computing capabilities; and even the realtime performance of a GPU varies with respect to factors such as kernel saturation and GPU occupancy, all of which pose a great challenges to load balancing. (2) Minimizing and overlapping communication is key to achieve high performance. (3) Reducing the CPU-GPU communication to the GPU-GPU communication further improves the communication and energy efficiency. Unfortunately, our study indicates the existing multi-GPU level-3 BLAS fail to optimize toward these factors, thereby delivering sub-optimal performance.

In this paper, we present the BLASX: a high-performance level-3 BLAS library for heterogeneous multi-GPU systems. We address the load balancing with a dynamic scheduling runtime, which handles task level workload variations, single GPU realtime performance variations and speed discrepancies among heterogeneous multi-GPUs. BLASX adopts a novel two level hierarchical tile caches to explore the tile temporal locality, in which we consider the GPU onboard RAM as the L1 tile cache and the combined multi-GPU RAMs as the L2 tile cache. The L1 tile cache minimizes global communication; and the L2 tile cache successfully reduces the CPU-GPU communication to the GPU-GPU communication. In implementing this hierarchical tile caches, we propose a new LRU algorithm to accommodate the asynchronous task progression and a new cache coherence protocol to ensure the data consistency on multi-GPUs. BLASX also optimizes the communication/computation overlapping on GPU streams so that the communication cost is negligible. Finally, BLASX offers backward compatibility to the vast existing CPU BLAS based applications; thereby all the details, such as workload balancing, data caching, communication overlapping and memory management, can be ignored by library users.

We evaluate BLASX on two multi-GPU systems, Everest and Makalu (TABLE II), against the related leading academic and industrial projects including cuBLAS-XT, SuperMatrix, MAGMA and PaRSEC. BLASX consistently outperforms the academic implementations on Everest with 3 NVIDIA Kepler K40c. In contrast to the highly optimized NVIDIA cuBLAS-XT, BLASX demonstrates on average 25% performance gain and 200% less communication volume. Makalu features 2 Kelper K40 and 2 Maxwell TITAN X. BLASX successfully tackles the heterogeneity and demonstrates linear speedup; whereas other libraries such as cuBLAS-XT, MAGMA and SuperMatrix suffers from poor scalability.

⁰BLASX is publicly available at <https://github.com/linnanwang/BLASX>

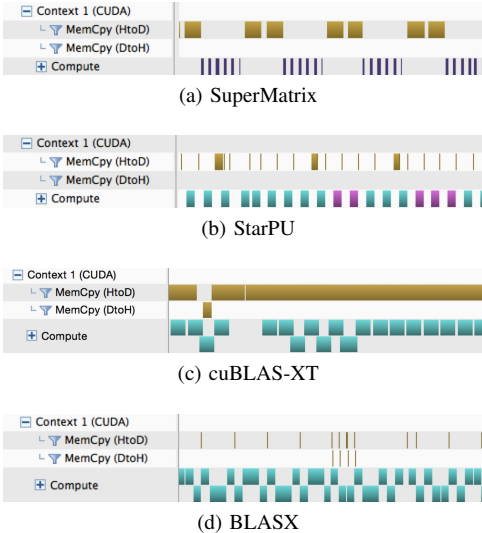


Fig. 1: A snapshot of single GPU DGEMM execution profile from SuperMatrix, StarPU, cuBLAS-XT and BLASX.

We organize the remaining paper as follows. Section II analyzes the background and related works; and section III briefly reviews the L3 BLAS tile algorithms. In Section IV, we elaborate the detailed design and implementations of BLASX including two level hierarchical tile caches and the scheduling runtime. We also present solutions to specific questions such as amortizing high frequency memory allocation and deallocation, communication and computation overlapping. The comprehensive evaluations of BLASX against existing state-of-art implementations are presented in the Section V. Finally, we conclude at Section VI.

II. BACKGROUND AND RELATED WORK

There are three levels of BLAS, divided with respect to the complexity of operations. Level-1 (L1) BLAS targets vector operations in $O(n)$ such as vector dot products and vector norms. Level-2 (L2) BLAS targets matrix-vector operations in $O(n^2)$ such as matrix-vector multiplication. Level-3 (L3) BLAS [1] targets matrix operations in $O(n^3)$ time such as matrix-matrix multiplications. The focus of this research is on L3 BLAS, which uses General Matrix Multiplication (GEMM) as the primary building block for the routines within the category. Therefore, the task of improving the performance of L3 BLAS can be reduced to the GEMM speed.

The massive but economic TFLOPS brought forth by the evolving GPU architectures drives interests in the various implementations of multi-GPU L3 BLAS. SuperMatrix [2] is one of the pioneers of matrix operation parallelization on SMP multicores, however it provides limited support on GPUs. The key insight of SuperMatrix is that a matrix can be factorized into a set of tiles. The Tomasolu algorithm [3] subsequently schedules these tiles in the out-of-order fashion. Fig. 1a demonstrates that SuperMatrix suffers from costly nonoverlapped CPU-GPU data transfers. StarPU provides a centralized interface to various accelerator technologies [4]. In contrast to Supermatrix, StarPU supports versatile scheduling algorithms such as work stealing [5] and priority scheduling [6] while requiring manual annotations to optimize under a specific problem. The insufficient communication/computation

overlapping and the low GPU saturation in Fig. 1b demonstrate the suboptimal DGEMM implementation in StarPU. MAGMA [7] is another multi-GPU linear algebra library with incomplete LAPACK and BLAS support. It is a heavily hand tuned library relying on a static load balancer, which degrades MAGMA’s performance on heterogeneous multi-GPU systems. Direct Acyclic Graph (DAG) scheduling has seen a revival in the recent years as it can naturally integrate with tile algorithms. ParSEC [8] is a leading DAG scheduling runtime for dense linear algebraic operations. Building DAGs at runtime and scheduling tasks within DAGs, however, can be a huge cost for the small scale L3 BLAS operations. ParSEC also assumes constant workload on each fine-grained task and constant speed on each GPU. It is possible to have workload variations and the GPU kernel saturation also affects the actual execution speed. In addition, ParSEC only exploits tile reusing within a single GPU; Caching on multiGPU memory spaces by taking advantages of GPU-GPU P2P communication still remains unexplored. None of the aforementioned libraries are backward compatible to legacy CPU BLAS. As an reaction to the market, NVIDIA released a commercial multiGPU L3 BLAS, cuBLAS-XT [9], declaring it to be backward compatible when using the NVBLAS wrapper. cuBLAS-XT consistently moves tiles on demand into GPU RAM so that it can compute a large scale problem with a few MB of GPU RAM. Although major communication is overlapped, it does not address tile caching; and this aggressive on demand communication pattern extremely overloads the PCI-E as shown by the contiguous yellow blocks in Fig. 1c.

In summary, these libraries cannot deliver the optimal performance due to following issues: 1) insufficient communication/computation overlapping subjects SuperMatrix and StarPU to suboptimal performance. 2) excessive communication in cuBLAS-XT overloads the PCI-E dragging down the overall performance. 3) low GPU occupancies in SuperMatrix and StarPU indicate partial GPU utilization. 4) efficient GPU-GPU P2P communication remains unexplored. We observe that the average throughput of CPU-GPU communication is 6.54 GB/S while the GPU-GPU is 7.80 GB/S. 5) static scheduling in the cuBLAS-XT and MAGMA cannot tackle the hardware heterogeneity. BLASX successfully resolves these issues as demonstrated in Fig. 1d; please refer to *Performance Evaluation* for detailed discussion.

III. A REVIEW OF L3 BLAS TILE ALGORITHMS

In this section, we give an overview of L3 BLAS tile algorithms. L3 BLAS is intended for $O(n^3)$ matrix operations including General Matrix Multiplication (GEMM), symmetric rank-k update (SYRK), symmetric rank-2k update (SYR2K), triangular matrix multiplication (TRMM), symmetric matrix multiply (SYMM), and triangular solve with multiple right hand side (TRSM). Since the Hermitian matrix multiplication (HEMM), Hermitian rank-k update (HERK), and Hermitian rank-2k update (HER2K) are the complex counterparts of GEMM, SYRK and SYR2K respectively, we omit their discussion in this paper.

A. Representing Matrix as Tiles

The tile algorithm logically partitions a matrix into its tiled representation. Given tile size T in a matrix of size $N \times M$, it creates $\lfloor N/T \rfloor \times \lfloor M/T \rfloor$ square tiles of size $T \times T$ and $(\lceil N/T \rceil \times \lceil M/T \rceil) - (\lfloor N/T \rfloor \times \lfloor M/T \rfloor)$ non-square tiles.

TABLE I. GEMM percentages at 3 different matrix sizes N.

Routines	N=5K	N=10K	N=20K
SYRK	74.5%	86.3%	92.8%
TRSM	68.5%	80.4%	89%
TRMM	69%	81.5%	92.8%
SYR2K	74.4%	85.4%	92.9%
SYMM	71.7%	84.9%	92.1%

Furthermore, the algorithm treats tiles, uniquely indexed by row and column, as the basic elements in a matrix in lieu of scalars. Operations on matrices are subsequently reduced to operations on tiles. As our focus is the L3 BLAS, we assume the tile indices of the output matrix are $[i, j]$, the tile indices of the matrix to the left side of multiply operator are $[i, k]$ and the tile indices of matrix to the right of multiply operator are $[k, j]$. Hence tile indices i and j uniquely identify a tile, C_{ij} , in the output matrix while the upper bound of k represents the computational intensity to solve the C_{ij} .

B. Traditional GEMM based L3 BLAS Tile Algorithms

The traditional tile implementation of L3 BLAS on the CPU relies on a highly optimized GEMM and a small amount of L1 and L2 BLAS [10] or other L3 BLAS routines. The following equations illustrate the none-transpose, upper triangular cases of L3 BLAS tile algorithms: GEMM, SYRK, TRSM, TRMM, SYR2K and SYMM, respectively:

$$C_{ij} = \alpha \sum_{k=0}^z A_{ik} B_{kj} + \beta C_{ij} \quad (1a)$$

$$C_{ij} = \alpha \sum_{k=0}^z A_{ik} A_{jk}^T + \beta C_{ij} \quad (1b)$$

$$C_{ij} = \alpha A_{ii}^{-1} \left(B_{ij} - \sum_{k=i+1}^z A_{ik} C_{kj} \right) \quad (1c)$$

$$C_{ij} = \alpha \sum_{k=i+1}^z A_{ik} C_{kj} + A_{ii} C_{ij} \quad (1d)$$

$$C_{ij} = \alpha \sum_{k=0}^z A_{ik} B_{jk}^T + \alpha \sum_{k=0}^z B_{ik} A_{jk}^T + \beta C_{ij} \quad (1e)$$

$$C_{ij} = \alpha \sum_{k=0}^i A_{ki}^T B_{kj} + \alpha \sum_{k=i+1}^z A_{ik} B_{kj} + \beta C_{ij} \quad (1f)$$

C. A simple trick to Matrix Transpose

The transpose of a tiled matrix requires a transpose on each tiles in addition to swapping the tiles A_{ij} and A_{ji} to be consistent with the definition of matrix transpose. The concept is as follows:

$$\begin{bmatrix} A_{00} & A_{01} \\ A_{10} & A_{11} \end{bmatrix} \begin{bmatrix} B_{00} & B_{01} \\ B_{10} & B_{11} \end{bmatrix}^T = \begin{bmatrix} A_{00} & A_{01} \\ A_{10} & A_{11} \end{bmatrix} \begin{bmatrix} B_{00}^T & B_{10}^T \\ B_{01}^T & B_{11}^T \end{bmatrix}$$

This simple trick significantly facilitates the matrix transpose. Rather than physically transposing the entire matrix, we can retrieve the tile A_{ji} and transpose the tile inside the BLAS kernel to implicitly transpose the matrix.

D. The GEMM Dominant L3 BLAS

TABLE I presents the GEMM percentages in L3 BLAS with respect to 3 square matrix sizes. The percentages of GEMM, as indicated in 1a to 1f, increase with the size of matrices to a point that the entire computation eventually

be dominated by the GEMM kernel, achieving GEMM-like performance.

IV. BLASX: A MULTI-GPU L3 BLAS LIBRARY WITH A LOCALITY AWARE DYNAMIC SCHEDULING RUNTIME

We organize this section as follows. We begin by introducing a set of new L3 BLAS tile algorithms for heterogeneous multi-GPUs. Subsection A elaborates the L3 BLAS task-ization; Subsection B elaborates a novel two-level hierarchical tile cache on multi-GPU RAMs; Subsection C elaborates our locality aware scheduling runtime covering load balancing, scheduling infrastructure, and scheduling strategies; Subsection D elaborates communication/computation overlapping and GPU out-of-core operations. In the end, we present a novel heap design to amortize the overhead introduced by high-frequency GPU memory allocation/deallocation.

Algorithm 1: A new L3 BLAS tile algorithm for heterogeneous multi-GPUs

Data: A, B and C
Result: C

```

1 begin
2   NoneBlockingTaskQueue( $TQ$ )  $\leftarrow$  init( $A, B, C$ )
3   CacheCoherenceProctol( $CCP$ )  $\leftarrow$  init()
4   for  $gpu \in GPU\ s$  do
5      $\lfloor$  SpawnThread(ComputingKernel, [ $TQ, CCP$ ])
6    $\rfloor$  AllThreadsJoin()
7
8 Function ComputingKernel ( $TQ, CCP$ )
9   BindToCore(self)
10  while  $TQ \neq \emptyset$  do
11    for  $RS \in$  ReservationStation( $RS$ ) do
12      if  $RS = \emptyset$  then
13         $task \leftarrow$ 
14          Dequeue( $TQ$ ) or WorkStealing()
15         $priority \leftarrow$  CalculatePriority( $task$ )
16         $RS \leftarrow \{task, priority\}$ 
17
18    StreamsSynch()
19    ReaderUpdate()
20    for  $k$  do
21      for  $task \in$  Top 4 Prioritized Tasks in RS do
22         $i \leftarrow task, j \leftarrow task$ 
23         $stream\_idx \leftarrow task$ 
24         $A_{ik} \leftarrow CCP(\&(task \rightarrow A_{ik}))$ 
25         $B_{kj} \leftarrow CCP(\&(task \rightarrow B_{kj}))$ 
26        SetStream( $stream\_idx$ )
27        AsyncBLAS( $A_{ik}, B_{kj}, C_{ij}$ )

```

Alg.1 describes the skeleton of the proposed L3 BLAS algorithms for heterogeneous multi-GPUs. Lines 1 to 6 indicate the general runtime procedures; and lines 8 to 25 indicate the GPU specifics during the computation. In lines 1 to 6, the runtime initializes a hierarchical tile cache and a global non-blocking task queue. Then a CPU thread is spawned for each GPU to submit instructions. The threads join together after the global task queue depletes. In lines 8 to 25, GPUs concurrently retrieve tasks and interleave them via multi-streams to overlap the communication during the asynchronous progression. The line 13 indicates two ways

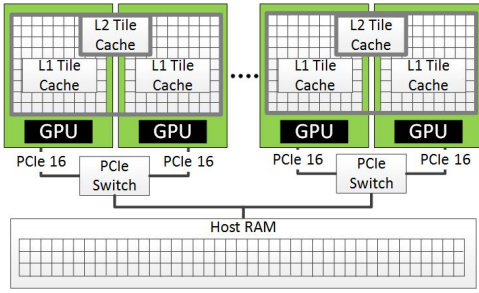


Fig. 2: The proposed two levels hierarchical tile caches. The L1 tile cache is the GPU onboard RAM; the L2 tile cache is the combined RAMs of GPUs on the same PCI-E switch. Each block holds a tile on a contiguous independent memory segment.

of task retrieval, either from global task queue or working task stealing. A GPU steals tasks from other Reservation Stations (RS), which only happens when the GPU exhausts tasks on RS while the global queue is also empty. Lines 22 and 23 reflect tile reuses with the proposed tile caches. Line 25 suggests an asynchronous L3 BLAS kernel invocation, the type of which is dictated by Eq. 1 given the tile indices i , j and k . Lines 18, 19 and 24 indicate the communication/computation overlapping. Although we implement this algorithm on NVIDIA GPUs, we can easily migrate it to work on other accelerator technologies such as Intel Xeon Phi and AMD FirePro.

A. Taskizing L3 BLAS

We define the task as solving a C_{ij} in Eq. 1. Tile algorithms yield the insight to systematically break down the output matrix C into a set of tiles C_{ij} , the computation of which, involves reading A_{ik} , B_{kj} , C_{ij} and an independent write of C_{ij} . Hence concurrently solving the C_{ij} is data hazards free. Eq. 1 also indicates that the workload of C_{ij} in non-GEMM routines varies according to the upper bound of k . In summary, a task has 3 notable properties by following definition:

- Reading the inputs for a task is data dependency free.
- Concurrent writing a task's output is data race free.
- The workload of each task varies.

Given a matrix C of size $M \times N$ and tile size T , the degree of parallelism is as follows:

$$\text{degree-of-parallelism} = \lceil M/T \rceil * \lceil N/T \rceil \quad (2)$$

In our implementation, a task holds the necessary metadata to solve a C_{ij} such as tile indices i , j and k , the dimensions of C_{ij} , and its host address. The runtime virtually slices a matrix and stores the tile metadata in tasks. Consequently, taskizing a L3 BLAS does not require significant additional memory.

B. Two Level Hierarchical Tile Caches

Fig. 2 demonstrates the structure of separate memory spaces on the multiGPU system. Each GPU equips with a private RAM; and CPUs share the host RAM. Nowadays, GPU RAM can be up to 12 GB while a single double precision matrix of size $32768 * 32768$ is 8.6 GB. The relatively small GPU RAM capacity limits the GPU in-core computing from handling the large scale L3 BLAS. One solution using tile algorithms is to dissect a large L3 BLAS into smaller ones, and solve them in succession. At each time, we move in tiles from the host on demand. Frequent GPU off-chip memory access, however, overloads the PCI-E and degrades the performance to be suboptimal. Meanwhile it is possible to reuse certain tiles

in separate tasks as indicated by Eq. 1. Therefore, exploiting the tile temporal locality by caching the most frequently used ones on the GPU RAM is necessary.

We present a novel two level fully associative tile caches in Fig. 2. The L1 tile cache is implemented using GPU onboard RAM; the L2 tile cache is implemented using the combined memory spaces of GPUs, which share the same I/O hub. The L1 tile cache hit enables direct tile reuse; the L2 tile cache hit reduces the CPU-GPU communication to GPU-GPU communication by retrieving the tile from the hardware adjacent GPU. The rationale of implementing the L2 cache are twofold: (1) GPU P2P communication better saturates PCI-E delivering at least 6 GB/s performance. [11] (2) The comparably faster GPU RAM reduces the latency of data fetching. Therefore it is more cost effective to retrieve a tile from a GPU than from the host RAM. To the best of our knowledge, BLASX is the first linear algebra library that considers such tile cache hierarchies on multi-GPU systems.

Algorithm 2: The ALRU Operations

Data: Tile_Host_Address (HA) and $ALRU$
Result: GPU_Address (GA)

```

1 Function Translate ( $ALRU, HA$ )
2    $LRUBlock(LB) \leftarrow ALRU.HashMap(HA)$ 
3   if  $LB = \emptyset$  then
4      $GA \leftarrow Malloc(TileSize)$ 
5     if  $GA = \emptyset$  then
6        $GA \leftarrow ALRU.Dequeue()$ 
7      $ALRU.Enqueue(HA, GA)$ 
8     return  $GA$  /* new tile cache */
9   else
10    return  $LB.GA$  /* cache hit */
11 Function Dequeue ()
12    $LRUBlock(LBEnd) \leftarrow ALRU.end$ 
13   while  $LBEnd \neq ALRU.begin$  do
14     if  $LBEnd.Reader = 0$  then
15       remove the  $LBEnd$  from the  $ALRU$ 
16     return  $LBEnd.GA$ 
17   else
18      $LBEnd \leftarrow LBEnd.Previous$ 
19 Function Enqueue ( $HA, GA$ )
20    $LRUBlock(LB) \leftarrow Malloc(LRUBlock)$ 
21    $LB.HA \leftarrow HA, LB.GA \leftarrow GA$ 
22    $LB.Reader \leftarrow 0$ 
23    $ALRU.HashMapInsert(HA, GA)$ 
24    $ALRU.InsertFront(LB)$ 

```

To implement the L1 tile cache, we need a LRU to discard the least frequently used tiles. Unfortunately the vanilla LRU algorithm [12] can not accommodate the asynchronous kernel launches in BLASX. Consequently, we propose the Approximate Least Recent Used (ALRU) to handle asynchronicities. Alg. 2 presents the three basic operations in the proposed ALRU. It adopts a reader (line 22) to track the tile usage. Specifically the reader of a tile is atomically incremented if a task need it. On the other hand, the reader is atomically decremented if a task releases the tile. We only update readers promptly after the synchronization point because that's the only place to inform the tile status (line 17 in Alg. 1). A

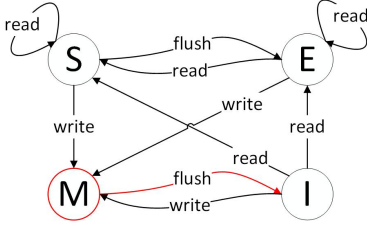


Fig. 3: The state transition diagram of MESI-X protocol in BLASX. The red M state is an ephemeral state, which immediately transits to I state by writing the tile back to host RAM.

reader equals 0 indicating no tasks using it; thereby it can be released in the ALRU. Since the runtime does not immediately synchronize readers in the asynchronous progress, it is possible to have nonzero reader on the least recent used tile. This deviates from the vanilla LRU policy by discarding the first approximate (as opposed to the exact) least recent used tile having the zero reader, which is reflected by lines 14-18 in Alg.2.

To implement the L2 tile cache, we need a cache coherence protocol to ensure the consistency of shared tiles in multiple places. We adopt the MESI-X cache coherence protocol, a variant of MESI protocol [13], to work for the BLASX’s particular context. Each ALRU associates with a specific GPU; The ALRUs all together reflect tile states in accordance with MESI-X protocol as follows: A tile is at E state if only a ALRU tracks it; A tile is at S state if multiple ALRUs track it; A tile is at I state if no ALRUs track it; A tile is at M state if a GPU writes a C_{ij} to it. Unlike the regular MESI protocol, we define the M state as an ephemeral state that writes back any tile in the state to the host RAM and sets the tile state immediately to I. Fig.3 demonstrates the state transition diagram of the proposed MESI-X.

C. Scheduling Infrastructure and Strategies

Our scheduling runtime achieves three specific goals: the proper load balancing on heterogeneous multi-GPUs and multi-CPUs, the efficient communication with locality aware scheduling and the sufficient overlapping of computation and communication. Fig.4 presents the scheduling infrastructure in our locality aware scheduling runtime, which consists of 4 major components:

1) *GPU Computation Thread*: a CPU thread to submit tasks for a specific GPU. To avoid the OS scheduling pre-emption, we bind the thread to a dedicated CPU core. The communication/computation overlapping requires at least 2 tasks concurrently running on streams; while Wei et al. [8] demonstrate no performance gain when using more than 4 streams. This leads us to adopt 4 concurrent tasks to overlap the computation/communication, which also explains the 4 streams used in Fig.4.

2) *CPU Computation Thread*: a CPU thread to submit tasks for the rest of CPU cores. Peng et al. proposes the hybrid tile layout to CPU Cores and GPUs due to the inherent devices’ performance differences [14]. We adopt the same concept but different approach. The CPU cores dequeue one task at each time and solve the task with a multithreaded BLAS kernel, where the tile is further factorized.

3) *Reservation Station (RS)*: a buffer designed to hold the upcoming tasks for a GPU. The runtime conducts work

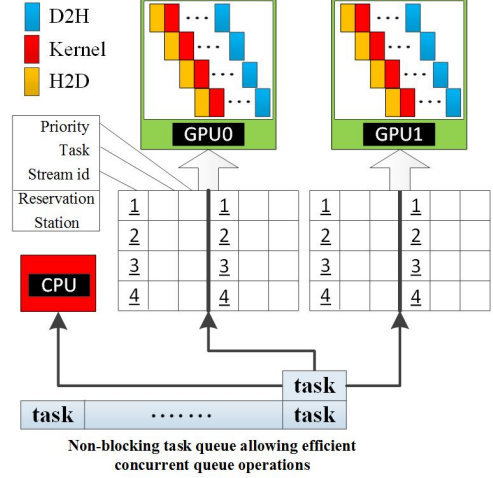


Fig. 4: The runtime infrastructure for our locality aware dynamic scheduler. G2H is the GPU to Host data transfer while H2G is the reverse.

stealing and priority scheduling on it. Each slot of a RS conveys a task priority, a task metadata, and a stream index.

4) *Non-blocking Task Queue*: It is a non-blocking queue allowing efficient concurrent dequeue and enqueue operations based on the algorithm proposed by Maged and Michael [15].

On heterogeneous systems, tasks can be executed on any computing device with load balancing being key to achieve optimal performance. In reality, it is possible to have task workload variation computed on the processors of various speeds. The two effects accentuate the uncertainty of processors on tasks consumption speed. One simple load balancing solution is to distribute tasks based on the inherent processors’ speeds, which is the case in ParSEC; the actual execution time, however, changes with the GPU kernel saturation and the actual tasks’ workload. Hence this solution may lead heavy tasks, however rare to clog the slower processor(s). Our load balancing scheme leverages the task-level workload and the processors’ real time speed to achieve the optimal performance. We treat GPUs about to entering idle states as a sign of demand, causing the thread to dequeue tasks. The key of our dynamic task-scheduling runtime is that processors simultaneously pull out tasks from the global non-blocking task queue by their demands. Specifically, faster processors consume more tasks and initiate more demands while the slower processors consume fewer and demand less. The load is thereby adjusted according to the real time demand of individual processors. The perfect scenario in this case is such that processors, regardless of speed difference, spend identical time on task execution without idling.

We adopt the work sharing and the work stealing to achieve this demand driven load balancing on the proposed runtime infrastructure. Lines 10 to 13 in Alg.1 indicate each GPU populates the affiliated RS either through global task queue or work stealing. The global non-blocking task queue simulates the work sharing by enabling concurrent task retrieval from multi-GPUs. Since the line 16 in Alg.1 is a synchronization point, a GPU will not demand tasks from RS unless it finishes current ones. Hence GPUs that demand more attempt to pull out more tasks from the queue. The work stealing intends to further improve the load balancing under the situation of

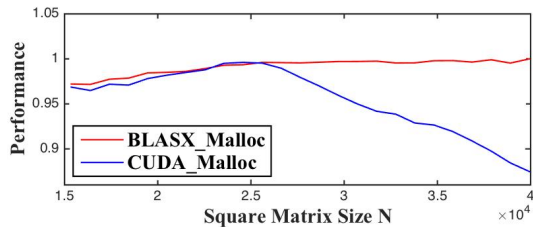


Fig. 5: Performance degeneration when increase the matrix size using CudaMalloc and CudaFree.

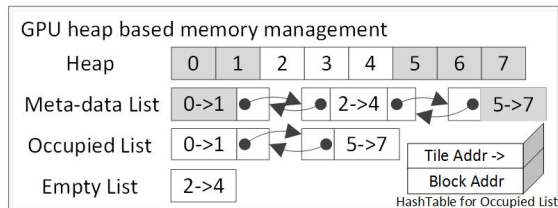


Fig. 6: A fast heap design to amortize the GPU memory allocation/deallocation overhead.

empty global task queue but full RS on GPUs. In this case, a underutilized GPU or CPU takes the initiative to steal a task from a overloaded RS, further balancing tasks at a finer level.

Prioritizing tasks with the better temporal locality lessens unnecessary communication. Lines 14, 15 and 19 in Alg.1 demonstrate task prioritization in the runtime. At each k , a GPU fetches top 4 prioritized tasks from the affiliated RS. The runtime refreshes the priorities in RS after new tasks coming in. The runtime populates tasks' priorities based on the extent of potential cache hits, which follows:

$$priority = \sum_{k=0}^z (f(\mathbf{A}_{ik}) + f(\mathbf{B}_{kj})) \quad (3a)$$

$$f(\mathbf{X}) = \begin{cases} 0, & \text{Otherwise} \\ 1, & \text{if L2 cache hit} \\ 2, & \text{if L1 cache hit} \end{cases} \quad (3b)$$

The tile locality has 3 scenarios: it hits the L1 tile cache; it hits the L2 tile cache and it is located at the host RAM. In terms of communication cost, there is no cost for L1 cache hit, and the L2 cache hit incurs less cost than retrieving the tile from the host.

D. Overlapping Computation with Communication

The CUDA stream is sequential operations executed in the issued order on the GPU with two notable properties. First, the operations on different streams can be simultaneously executed within the same physical device. This property enables the communication/computation overlapping via moving the data on one stream while executing kernels on another one. Secondly, streams can divide the GPU processing power between a few tasks by allocating segments to each task in turn. With these two properties, a tight interleaving of tasks on multiple streams can render the actual communication cost trivial.

L3 BLAS tile algorithms indicate that a task essentially involves $k \in [1, z]$ steps of kernel execution. The runtime overlaps the communication/computation by interleaving tasks as follows: First, the RS directly maps top 4 prioritized tasks

TABLE II. The system configuration of experimental machines

	System Configuration	
	Everest	Makalu
OS	CentOS v. 6.3	Ubuntu Server 14.04
GPU	3 Kelper K40	2 Kelper K40 and 2 Maxwell Titan X
CPU	2×Xeon E5 4655 V3	2 Xeon E5 1620 V3
RAM	64 GB DDR3	64 GB DDR3
CUDA	v 6.5	v 7.0
Compiler	GCC 4.4.7	GCC 4.8.2
CPU BLAS	OpenBLAS v 1.13	OpenBLAS v 1.13

onto 4 CUDA streams. Second, the runtime executes each step, k , on all streams such that tasks in the step are computed before advancing to the next step (line 19-25 Alg.1), which is guaranteed by the sequential execution feature of CUDA stream. Solving a step of tasks involves data transfer of the required tiles (if cache miss) followed by kernel executions. As tasks progress on multiple streams in this way, the data transfer on a stream eventually overlaps with the kernel execution on another one. In sum, we can consider the overall execution time to be the sum of kernel execution time, plus initial tile move in, and plus final tile move out. This negligible communication cost enables the input and output matrices to reside on the host memory. Consequently we claim our GPU operations are out-of-core.

E. Amortize GPU Memory Allocation/Deallocation Overhead

GPUs require memory allocation for tiles move-in and deallocation for tiles move-out. Increasing the computation scale leads to the performance deterioration due to the significant overhead of memory allocation/deallocation. Fig. 5 presents the performance degeneration with CUDA's native memory management utilities such as cudaMalloc and cudaFree. As a consequence, we implement a fast heap based GPU memory management utilities, BLASX_Malloc, to alleviate this issue. The core concept of it is to amortize the allocation/deallocation overhead by adopting a big chunk of GPU memory as the preallocated heap.

Fig. 6 presents the basic scheme of the proposed heap design, which consists of a meta-data list, a occupied list and an empty list. A node in the meta-data list traces the length of memory segment and its occupation status. Each block of the occupied and empty list tracks the allocated segment and the free segment respectively. The dynamics of this heap is as follows: During the allocation, the heap searches for the first node with enough memory in the empty list, which is subsequently split into two nodes. One for the occupied list recording the allocated memory; The other for the empty list recording the residual memory. During the deallocation, the runtime locates the segment in the occupied list with a hashtable. If either the node's left or right neighbors are contiguous with the node in terms of memory, they merge together. Then the segment is marked as free and placed back to empty list afterwards. Fig. 5 demonstrates our heap based method effectively amortizes the memory allocation and deallocation overhead.

V. PERFORMANCE EVALUATION

In this section, we present comprehensive evaluations of our L3 BLAS routines. We conducted the experiments on two shared memory machines Everest and Makalu, the specifications of which are included TABLE II.

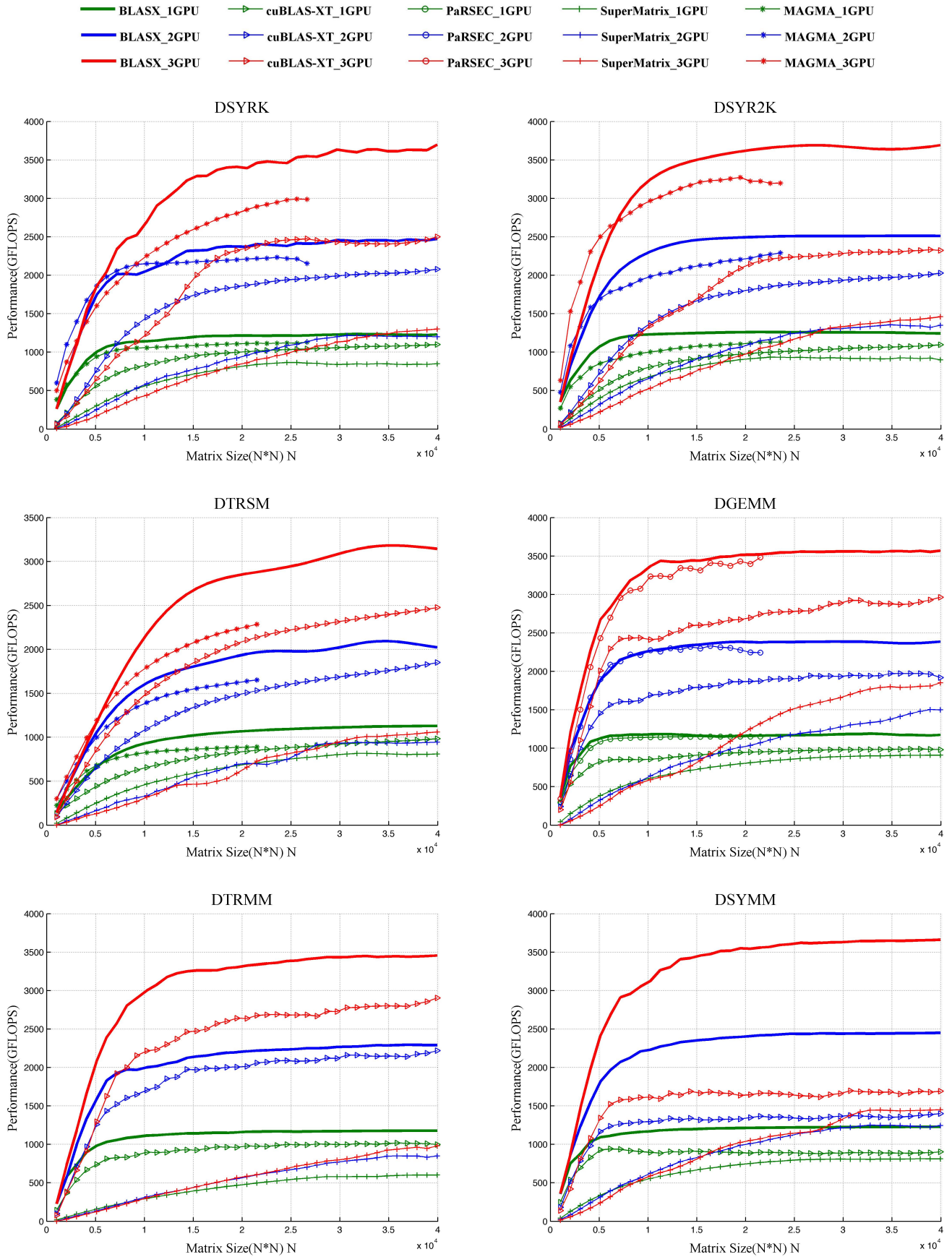


Fig. 7: The comprehensive benchmarks of double precision L3 BLAS on Everest. BLASX demonstrates superior performance than state-of-art commercial product cuBLAS-XT and academic related projects such as MAGMA and SuperMatrix. The out-of-core GPU operations in BLASX enables larger scale GPU computing than does the in-core GPU operations by PaRSEC and MAGMA.

TABLE III. The average parallel efficiency of various implementations with input square matrix $N \in [1024, 39936]$ on Everest.

Routines	BLASX	PaRSEC	MAGMA	cuBLAS-XT	SuperMatrix
DSYRK	85.54%	N/A	N/A	64.21%	33.33%
DTRSM	81.58%	N/A	77.3%	77.27%	30.72%
DTRMM	88.99%	N/A	N/A	82.11%	38.96%
DSYMM	90.36%	N/A	N/A	57.96%	43.42%
DGEMM	93.53%	92.85%	N/A	89.85%	46.22%
DSYR2K	85.54%	N/A	79.58%	64.21%	34.70%

TABLE IV. The average throughput of Direct Memory Access(DMA) engine.

	Bidirectional Host and GPU	GPU to GPU
Throughput	6.54 GB/s	7.8 GB/s

A. The Comprehensive L3 BLAS Benchmark

We evaluate performance against a commercial product cuBLAS-XT and seminal academic libraries such as SuperMatrix, PaRSEC and MAGMA. We setup benchmarks on the machine Everest (TABLE II) using double precision L3 BLAS routines. The memory range of input or output matrices is page locked to expedite PCI-E transfer; and the time spent on page-locking is excluded from performance metric. The α and β are two random float constants; other parameters such as *UPLO*, *SIDE*, *TRANS* and *DIAG* are ensured to be same in each comparison. The input matrix size N starts from 1024 to 39936 at increments of 1024. The performance data are from the average of 3 runs; execution order of BLASX, cuBLAS-XT, MAGMA, SuperMatrix and PaRSEC is randomized to eliminate the potential ordering influence.

Fig.7 demonstrates the comprehensive benchmarks on Everest. In single GPU benchmarks, the mean performance of BLASX converges to 92.68% of the in-core cuBLAS DGEMM peak; whereas the average performance of PaRSEC, MAGMA, cuBLAS-XT and SuperMatrix attains 91.10%, 81.28% , 79% and 63.99% of in-core cuBLAS DGEMM peak respectively. Even though PaRSEC achieves comparable performance, its GPU in-core operation limits PaRSEC to handle matrix sizes $N > 22528$ as the required memory, $22528 * 22528 * 8 * 3 = 12.18$ GB, is beginning to exceed the GPU RAM 12 GB capacity. This also explains partial benchmarks on the MAGMA DSYR2K and DTRSM. The sufficient GPU communication/computation overlapping is one of predominant factors to the high performance of BLASX. Whereas Supermatrix follows a simple fork and join model blocking kernel launches until the on demand data is transferred. The non-overlapped communication in SuperMatrix incurs too much latency to delivery comparable performance. Hence we omit its discussion in the rest of paper.

BLASX demonstrates linear speedups and the highest scalability under multiGPU configurations. Fig.7 indicates performances increase with the matrix size and reaches a plateau after $N > 15000$. At the matrix size 16384, the DSYR2K speedup of BLASX, cuBLAS-XT, MAGMA on two GPUs are 1.99x, 1.83x, 1.91x; and the triple GPU speedup are 2.91, 2.16, 2.88. However, real world applications often entail small scale matrix $N < 15000$. Measuring parallelizations at various matrix sizes is more convincing than concluding the speedup

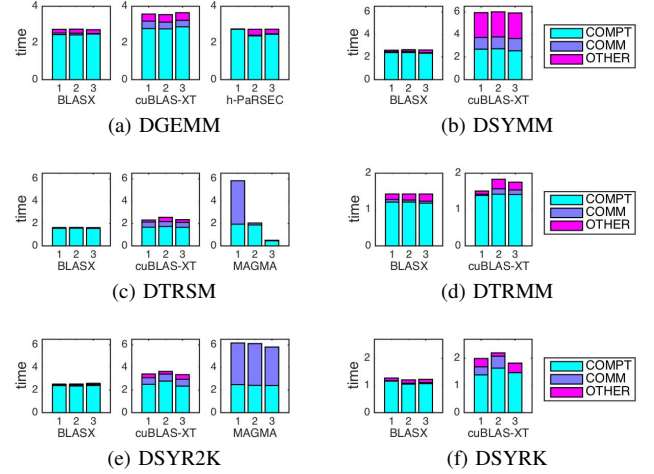


Fig. 8: The execution time profile (classified into COMPT, COMM and OTHER) at the square matrix size $N = 16384$ on Everest. The horizontal indices 1, 2, 3 represents GPU_1, GPU_2 and GPU_3.

at a particular matrix size. Since the parallel efficiency is a performance metric to describe the scalability at a specific problem size N , we calculate the average parallel efficiency based on 39 matrix sizes $N \in [1024, 39936]$ to yield a global insight about scalabilities at various matrix sizes; and we adopt forward padding to partial benchmarks in MAGMA and PaRSEC. In TABLE III, BLASX outperforms the second best alternatives at the average rate of 5%. Particularly BLASX DSYMM is 32.4% higher than the second best implementation by cuBLAS-XT. There are 4 major factors that contribute to the success of BLASX, which are 1) the demand-driven load balancing, 2) the seamless GPU occupancy, 3) the significantly less communication volume and 4) the efficient GPU-GPU P2P communication. We investigate each factors as follows.

First, our demand-driven dynamic load balancing is key to the BLASX high performance. In Fig.8, we dissect each GPU execution profiles into 3 major components—the computation (COMPT), the unoverlapped communication (COMM), the synchronization and free gaps among kernel launches (OTHER). A typical ideal scheduler allows each GPUs, regardless of differences, to spend identical time during the execution. Fig.8 indicates that dynamic schedulers employed by BLASX and PaRSEC are better than static schedulers by MAGMA and cuBLAS-XT. For example, the average elapsed time differences between the fastest GPU and the slowest GPU of cuBLAS-XT and BLASX are 0.2961 and 0.0391 seconds; and the same metric for MAGMA (only count COMM) and BLASX is 0.7837 and 0.0457 seconds. The DGEMM of PaRSEC and BLASX attains comparable performance of 0.0252 and 0.0285 seconds.

Second, the seamless GPU occupancy enables BLASX to fully saturate each GPU. In Fig.8, BLASX demonstrates the least non-computation cost (OTHER+COMM). The communication is counted toward latency if it is not overlapped. The average communication latency of BLASX is 0.0575s while cuBLAS-XT is 0.4917s. The difference is largely due to the significantly reduced communication volume and the seamless stream-level overlapping and kernel launches. OTHER

TABLE V. The communication volume(in MB) of L3 BLAS routines at the input square matrix size $N = 16384$.

MB	DGEMM			DSYMM	
	BLASX	cuBLAS-XT	h-PaRSEC	BLASX	cuBLAS-XT
GPU1	6895	24528	7563	5628	18865
GPU2	1811+4768	24243	7160	1249+5318	18865
GPU3	721+4462	24243	6160	343+3758	18102

MB	DTRSM			DTRMM	
	BLASX	cuBLAS-XT	MAGMA	BLASX	cuBLAS-XT
GPU1	2751	12985	15130	4966	8885
GPU2	981+4622	12792	2768	1694+4353	2020
GPU3	300+2575	12876	1587	327+2365	8922

MB	DSYR2K			DSYRK	
	BLASX	cuBLAS-XT	MAGMA	BLASX	cuBLAS-XT
GPU1	7281	15910	5738	4278	12314
GPU2	2231+5905	15910	5720	1363+3410	12834
GPU3	1308+2969	15900	5720	1213+2536	11492

† The red represents the volume of GPU to GPU communication.
 ‡ The black represents the volume of bidirectional Host to Device communication.
 ● The Peer access is only available between GPU2 and GPU3 on the machine Everest.

includes synchronization latency and the minor GPU idle gaps among kernel launches. The synchronization is necessary to ensure the mathematical rigorousness; and idle gaps depend on the tightness of kernel launches on multistreams. Increasing streams, as demonstrated by Wei et al [8], improves the GPU saturation by reducing those gaps. BLASX dynamically interleaves tasks over multiple streams, while cuBLAS-XT adopts two.

Third, the hierarchical tile caches in BLASX dramatically diminish the communication volume. According to TABLE V, the average communication volume of cuBLAS-XT, 15143 MB, is 2.95 times of BLASX, 5132 MB. The L1 tile cache of BLASX exploits the tile temporal locality to minimize global communication, which is not the case for cuBLAS-XT. The increasing gaps among the GPU clock frequency (1.43 TFLOPS on K40c), GPU memory bandwidth (288 GB/sec on K40c) and PCI-E bandwidth (31.51 GB/s v4.0 x16) identify GPU off-chip memory access extremely expensive. Consequently, the excessive data transfer of cuBLAS-XT incurs a huge latency penalty to its performance. The DGEMM data also indicates that BLASX (6219 MB) saves 12% communication over PaRSEC (6961 MB).

Finally, reducing the CPU-GPU communication to the GPU-GPU communication further improves the communication efficiency of BLASX. One of the defining features of BLASX is the implementation of L2 tile caches, the purpose of which is to retrieve tiles from hardware adjacent GPUs under L1 misses. TABLE IV justifies our L2 tile cache proposal indicating that the average GPU-GPU data transfer is 19.27% faster than the CPU-GPU transfer. We highlight the GPU-GPU communication volume in TABLE V. The interGPU communication only happens between GPU2 and GPU3 as only they share the same PCI-E switch on Everest. We expect the efficient GPU-GPU communication eventually dominating with more GPUs available on the system.

Fig.9 presents the DGEMM CPU performance of cuBLAS-XT and BLASX on the machine Makalu. We sample the CPU contribution by taking the difference of CPU enabled DGEMM to CPU disabled DGEMM under same scenarios. Our runtime automatically assign tasks to CPU; hence the performance is

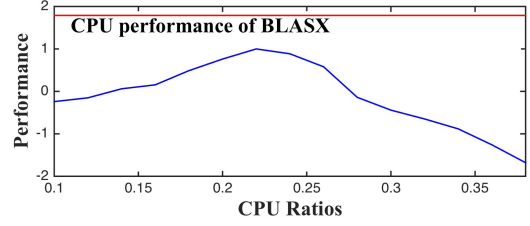


Fig. 9: The CPU performance of cuBLAS-XT and BLASX at various CPU ratios.

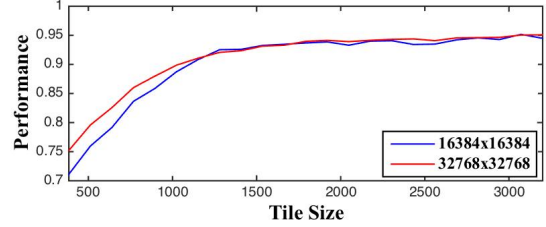


Fig. 10: The performance variations with respect to different tile sizes on Everest.

represented with a horizontal line. Fig.9 indicates the CPU contribution of BLASX is 78% faster than the best case in cuBLAS-XT. The downtrend in the figure also suggests an improperly chosen CPU ratio overloads the CPU at the expense of GPUs.

B. The Only Tuning Parameter—Tile Size

We strive to develop a portable L3 BLAS library that delivers the optimal performance on different platforms with the least effort from users. In BLASX, the tile size is the only tuning parameter. Generally a large tile size reduces the degree of parallelism while a small tile size poorly saturates the GPU and PCI-E. The ideal tile size is a result of trade-off among GPU saturation, PCI-E efficiency and available parallelism. Fig. 10 demonstrates the impact of tile size on the overall DGEMM performance at two matrix sizes. The performance increases with tile size and reaches a plateau eventually. In this case, we choose the tile size 1024×1024 for benchmarks on Everest.

C. Applications

BLASX intends to provide multiGPU performance boost by directly replacing the CPU based alternatives. Libraries such as MAGMA, h-PaRSEC and StarPU requires extensive changes on the legacy code to comply with standards while cuBLAS-XT requires commercial licenses without delivering a proportional increase of performance. In this section, we present a few applications of BLASX as follows:

a) Caffe [16] is one of the most popular deep learning frameworks nowadays, in which BLAS computes the image convolution [17], forwards and backwards passes of densely connected layers [18]. We built a CPU version of Caffe and changed the BLAS linkage to BLASX. An Artificial Neural Network (ANN) of architecture, $3072 \rightarrow 16384 \rightarrow 16384 \rightarrow 10$, was trained with CIFAR-10 dataset [19] to classify images in 10 categories. We used Caffe’s benchmark utilities to measure the average elapsed time for a forward and backward passes on the machine Makalu. The experiment data demonstrates that BLASX accelerates ANN training up to 2.48 W.R.T Caffe GPU training and 62.3 W.R.T Caffe CPU training. In terms

TABLE VI. The exemplary performance boost of MATLAB SIMULINK libraries while using BLASX on Everest.

command	Description	Speedup
$\mathbf{A} * \mathbf{B}$	matrix multiplication in single precision.	12.75x
$\mathbf{A} * \mathbf{B}$	matrix multiplication in double precision.	8.27x
nmmf	factorize the \mathbf{A} into nonnegative factors \mathbf{W} and \mathbf{H} .	6.72x
rotatefactors	rotates the \mathbf{A} to maximize the varimax criterion.	5.83x
lsqlin	solves the linear system in the least-squares sense	3.09x

of model parameters, the Caffe’s single GPU training can accommodate up to $1.5 * 10^9$ parameters on a 12 GB GPU. BLASX, however, enables a model of $3.2 * 10^{10}$ parameters on a multiGPU server with 256 GB host RAM. Please refer to our poster [20] for more details¹.

b) MATLAB, R and Octave are renowned technical computing languages widely used in academia and industry. These scientific languages offload the primitive matrix or vector operations to the BLAS to ensure the performance. Users can integrate BLASX with MATLAB by simply exporting the environment variable BLAS_VERSION to the location of BLASX. Although MATLAB has the GPU computing toolbox, it requires users to manually manage the data on the GPU yet without multiGPU support. BLASX elegantly resolves these issues with its underlying dynamic runtime. Table VI presents a few exemplary instances of MATLAB’s SIMULINK libraries while using BLASX. There are additional vast applications of BLASX such as finding the shortest path in a graph, the topology optimization [22] and finite element analysis in structure mechanics [23].

VI. CONCLUSION

Existing L3 BLAS libraries such as PaRSEC, MAGMA, Supermatrix, cuBLAS-XT suffers from issues such as backward compatibility, insufficient communication/computation overlapping, inefficient communication and poor scalability. In this paper, we design and implement BLASX, a suite of L3 BLAS, that delivers the best L3 BLAS performance on heterogeneous multiGPU systems. We introduce a novel two level hierarchical tile cache to reduce the global communication; Our locality aware scheduling runtime perfectly balances the load across heterogeneous GPUs and CPUs. We optimized communication/computation overlapping on streams to renders trivial communication cost; thereby BLASX computes in a out-of-core fashion that insures input and output data always remains on the host RAM. Extensive benchmarks demonstrate that BLASX consistently outperforms the leading industrial and academia related projects in terms of performance, scalability, and communication efficiency. More importantly, BLASX requires the least effort from users to integrate with the vast amount of legacy BLAS based applications.

REFERENCES

[1] Dongarra, Jack J., et al. "A set of level 3 basic linear algebra subprograms." ACM Transactions on Mathematical Software (TOMS) 16.1 (1990): 1-17.

[2] Chan, Ernie, et al. "Supermatrix: a multithreaded runtime scheduling system for algorithms-by-blocks." Proceedings of the 13th ACM SIGPLAN Symposium on Principles and practice of parallel programming. ACM, 2008.

[3] Tomasulo, Robert M. "An efficient algorithm for exploiting multiple arithmetic units." IBM J. Res. Dev (1995): 13-21.

[4] Augonnet, Cdric, et al. "StarPU: a unified platform for task scheduling on heterogeneous multicore architectures." Concurrency and Computation: Practice and Experience 23.2 (2011): 187-198.

[5] Blumofe, Robert D., and Charles E. Leiserson. "Scheduling multi-threaded computations by work stealing." Journal of the ACM (JACM) 46.5 (1999): 720-748.

[6] Leung, Joseph Y-T., and Jennifer Whitehead. "On the complexity of fixed-priority scheduling of periodic, real-time tasks." Performance evaluation 2.4 (1982): 237-250.

[7] Nath, Rajib, et al. "Optimizing symmetric dense matrix-vector multiplication on GPUs." Proceedings of 2011 International Conference for High Performance Computing, Networking, Storage and Analysis (SC). ACM, 2011.

[8] Wu, Wei, et al. "Hierarchical DAG Scheduling for Hybrid Distributed Systems." 29th IEEE International Parallel and Distributed Processing Symposium. 2015.

[9] developer.nvidia.com/cublasxt

[10] Goto, Kazushige, and Robert Van De Geijn. "High-performance implementation of the level-3 BLAS." ACM Transactions on Mathematical Software (TOMS) 35.1 (2008): 4.

[11] Schroeder, Tim C. "Peer-to-peer and unified virtual addressing." GPU Technology Conference, NVIDIA. 2011.

[12] Kdzierski, Kamil, et al. "Adapting cache partitioning algorithms to pseudo-lru replacement policies." Parallel & Distributed Processing (IPDPS), 2010 IEEE International Symposium on. IEEE, 2010.

[13] Sweazey, Paul, and Alan Jay Smith. "A class of compatible cache consistency protocols and their support by the IEEE futurebus." ACM SIGARCH Computer Architecture News. Vol. 14. No. 2. IEEE Computer Society Press, 1986.

[14] Song, Fengguang, Stanimire Tomov, and Jack Dongarra. "Enabling and scaling matrix computations on heterogeneous multi-core and multi-GPU systems." Proceedings of the 26th ACM international conference on Supercomputing. ACM, 2012.

[15] Michael, Maged M., and Michael L. Scott. "Simple, fast, and practical non-blocking and blocking concurrent queue algorithms." Proceedings of the fifteenth annual ACM symposium on Principles of distributed computing. ACM, 1996.

[16] Jia, Yangqing, et al. "Caffe: Convolutional architecture for fast feature embedding." Proceedings of the ACM International Conference on Multimedia. ACM, 2014.

[17] Chellapilla, Kumar, Sidd Puri, and Patrice Simard. "High performance convolutional neural networks for document processing." Tenth International Workshop on Frontiers in Handwriting Recognition. Suvisoft, 2006.

[18] Rumelhart, David E., Geoffrey E. Hinton, and Ronald J. Williams. "Learning representations by back-propagating errors." Cognitive modeling 5 (1988): 3.

[19] Krizhevsky, Alex, and Geoffrey Hinton. "Learning multiple layers of features from tiny images." (2009).

[20] Wang, Linnan, et al. "Large Scale Artificial Neural Network Training Using MultiGPUs" SC poster (2015).

[21] Seidel, Raimund. "On the all-pairs-shortest-path problem in unweighted undirected graphs." Journal of computer and system sciences 51.3 (1995): 400-403.

[22] Bendse, Martin P., and Ole Sigmund. "Topology Optimization." (2009): 3928-3929.

[23] Szabo, Barna Aladar, and Ivo Babuka. Finite element analysis. John Wiley & Sons, 1991.

¹The CPU activation of Caffe is a single thread function, which is not efficient. We modified the function to be multithreaded to benchmark the results.